Accepted Manuscript

A novel fluorescence biosensor for sensitivity detection of tyrosinase and acid phosphatase based on nitrogen-doped graphene quantum dots

Zhengyi Qu, Weidan Na, Xiaotong Liu, Hua Liu, Xingguang Su

PII: S0003-2670(17)31152-2

DOI: 10.1016/j.aca.2017.10.010

Reference: ACA 235481

To appear in: *Analytica Chimica Acta*

Received Date: 12 July 2017

Revised Date: 29 September 2017

Accepted Date: 5 October 2017

Please cite this article as: Z. Qu, W. Na, X. Liu, H. Liu, X. Su, A novel fluorescence biosensor for sensitivity detection of tyrosinase and acid phosphatase based on nitrogen-doped graphene quantum dots, *Analytica Chimica Acta* (2017), doi: 10.1016/j.aca.2017.10.010.

A novel fluorescence biosensor for sensitivity detection of tyrosinase and acid phosphatase based on nitrogen-doped graphene quantum dots

Zhengyi Qu, Weidan Na, Xiaotong Liu, Hua Liu and Xingguang Su*

Department of Analytical Chemistry, College of Chemistry, Jilin University, Changchun 130012, P.R. China

*Corresponding author: Xingguang Su

Tel.: +86-431-85168352

E-mail address: suxg@jlu.edu.cn

ABSTRACT

In this paper, we developed a sensitive fluorescence biosensor for tyrosinase (TYR) and acid phosphatase (ACP) activity detection based on nitrogen-doped graphene quantum dots (N-GQDs). Tyrosine could be catalyzed by TYR to generate dopaquinone, which could efficiently quench the fluorescence of N-GQDs, and the degree of fluorescence quenching of N-GQDs was proportional to the concentration of TYR. In the presence of ACP, L-Ascorbic acid-2-phosphate (AAP) was hydrolyzed to generate ascorbic acid (AA), and dopaquinone was reduced to L-dopa, resulting in the fluorescence recovery of the quenched fluorescence by dopaquinone. Thus, a novel fluorescence biosensor for the detection of TYR and ACP activity based on N-GQDs was constructed. Under the optimized experimental conditions, the fluorescence intensity was linearly correlated with the concentration of TYR and ACP in the range of 0.43 to 3.85 U mL^{-1} and 0.04 to 0.7 mU mL^{-1} with a detection limit of 0.15 U mL^{-1} and 0.014 mU mL^{-1}, respectively. The feasibility of the proposed biosensor in real samples assay was also studied and satisfactory results were obtained.

Key words: Graphene quantum dots; Tyrosinase; Acid phosphatase; Fluorescence biosensor

1. Introduction

Enzymes known as nature's catalysts could efficiently catalyze almost all biochemical processes in a controlled manner and precise specificity. This has made enzymes of considerable interest for utilizing in the construction of biosensors. Recently, enzyme-based biosensors, as an alternative to the conventional analytical methods, have been generally considered as simple and sensitive technique for selectively detecting target analytes [1].

Tyrosinase (TYR) is a typical polyphenol oxidase, copper-containing enzyme which is ubiquitously distributed in nature [2]. It mainly functions as catalyzing the hydroxylation of phenolic substrates to catechol derivatives, and further oxidizing the catechol derivatives to ortho-quinone products [3, 4]. TYR was first characterized in mammals for their role in the development of melanomas, and for their implication in pigmentation troubles such as albinism and vitiligo [5]. In humans, melanin is responsible for the colouring of skin and hair, and helps to protect the skin from the damage caused by ultraviolet radiation. However, excessively high levels of melanin can cause various dermatological disorders such as melasma, age spots and sites of actinic damage [6]. The melanin biosynthesis process: TYR oxidizes tyrosine to form L-3, 4-dihydroxyphenyl-alanine (L-dopa) and further oxidizes L-dopa to form dopaquinone. The resulting reactive ortho-quinones polymerise to melanin [7]. Additionally, because of its major effect on dopamine neurotoxicity, TYR imbalance may also cause Parkinson’s disease in association with neurodegeneration [8, 9]. Thus, sensitive detection of TYR activity is of great urgency to biomedical diagnosis.

Acid phosphatase (ACP), as a ubiquitous digestive enzyme, can catalyze the hydrolysis of phosphate monoester to release phosphate groups during digestion under acidic condition [10]. It is located primarily in a variety of mammalian tissues and fluids such as the prostate, liver, spleen, and kidney, blood, saliva, etc [11, 12]. An abnormal level of serum ACP has proven to be associated with several diseases, such as prostate cancer, hepatitis, thrombophlebitis, kidney disease hyperparathyroidism and multiple myelom [10, 11, 13]. As a result, ACP is always considered as an important serum marker for related disease and a useful prognostic indicator. Thus, the rapid and convenient analysis of ACP in blood is of particular importance. ACP has been detected using several methods based on enzymatic catalysis, including immunoassay [14], chromatographic [15], and electrochemical methods [16]. Although these methods offer

reasonable sensitivities, accurately quantify the amount of acid phosphate. However, some ACP assays are time-consuming or have poor reproducibilities, some require sophisticated instrumentation and expensive equipments [17, 18]. Fluorescence methods for ACP assay offer new alternatives, because they are rapid, continuous and occur in real time. But there are a few fluorescent assays for ACP detection, and fluorescent indicators used were mainly focused on organic dyes and fluorescent polymers [19].

In recent years, Graphene quantum dots (GQDs) have aroused tremendous research interest due to their extraordinary optical and electronic properties, which including low toxicity, unique photoluminescence, excellent solubility, high biocompatibility and robust chemical inertness. These emerging properties of GQDs make them more suitable for cellular imaging, drug delivery, disease diagnosis, especially as a fluorescence probe in biomedical detection [20，21].

Herein, we constructed a sensitive fluorescence biosensor for tyrosinase (TYR) and acid phosphatase (ACP) activity detection based on nitrogen-doped graphene quantum dots (N-GQDs). As shown in **Scheme 1**, tyrosine could be catalyzed by TYR to generate dopaquinone, which could efficiently quench the fluorescence of N-GQDs. The decrease in the fluorescence intensity of N-GQDs was directly related to the amount of TYR. Furthermore, we designed an assay for ACP based on the hydrolysis of AAP by ACP. In the presence of ACP, AAP could be hydrolyzed to generate AA, which could reduce dopaquinone, and resulting in the fluorescence recovery of N-GQDs. The recovery in the fluorescence of N-GQDs was directly related to the amount of ACP. Therefore, a novel, convenient and sensitive fluorescence biosensor for TYR and ACP activity detection based on N-GQDs has been established.

Scheme 1

2. Experimental

2.1 Chemicals and materials

Citric acid ($C_6H_8O_7.H_2O$), ammonia solution ($NH_3.H_2O$, 25.0-28.0%) and hydrochloric acid (HCl, 36.0–38.0%) were purchased from Beijing Chemical Works. Ascorbic acid (AA), 2-amino-2-hydroxymethyl-1,3-propanediol (Tris), cholesterol, glucose, tyrosine, tryptophan, arginine, threonine and phenylalanine were purchased from Beijing Dingguo Biotechnology Co.,

Ltd. Sodium L-ascorbyl-2-phosphate (AAP) was purchased from Dalian Meilun Biotech Co., Ltd. Tyrosinase (TYR) and acid phosphatase (ACP) were obtained from TCI (Shanghai) Development Co., Ltd and kept in a freezer at below -20°C. KCl, $CaCl_2$ and $MgCl_2 .6H_2O$ were obtained from Tianjin Guangfu Institute of Fine Chemicals. Human serum albumin (HSA), pepsin (1:3000), trypsin (1:250), uricase, glucose oxidase and lysozyme were obtained from Sino-American Biotechnology Co. Ltd. All chemicals used were at least of analytical reagent grade and used without further purification. The deionized water we used in all experiments had a resistivity higher than 18 MΩ cm^{-1}. The 0.1 mol L^{-1} Tris–HCl buffered solution (pH 6.2) was used as the medium for detection process. The human serum was obtained as a gift from the university hospital.

2.2 Instrumentation

Fluorescence spectra were measured with a Shimadzu RF-5301 PC spectrofluorophotometer (Shimadzu Co., Kyoto, Japan) equipped with a xenon lamp using right-angle geometry. Ultraviolet absorption spectra were carried out on Varian GBC Cintra 10e UV-visible Spectrophotometer. A 1 cm path-length quartz cuvette was used in the measurements above. FT-IR spectra were recorded with a Bruker IFS66V FT-IR spectrometer equipped with a DGTS detector. All pH value measurements were performed with a PHS-3C pH meter (Tuopu Co., Hangzhou, China).

2.3 Synthesis of nitrogen-doped graphene quantum dots

N-GQDs were synthesized according to a modified synthetic method in the literature [22]. The N-GQDs were synthesized by hydrothermal treatment of citric acid (as the carbon source) and ammonia solution (as the nitrogen source). In a typical synthesis procedure, 0.012 g of citric acid was dissolved in 12 mL of deionized water and then mixed with 1.5 mL of ammonia solution under vigorous stirring to form a transparent solution. Then the mixture was transferred into a 25 mL Teflon-lined stainless steel autoclave and heated at 200°C for 3 h. After the reaction, the reactor was cooled down to ambient temperature naturally. Then, dialyzed against deionized water using a dialysis membrane with a molecular weight cutoff 3500 Da for 8 h (changing deionized water every 4 h) to remove unreacted raw materials and low molecular weight by-products. Finally, the obtained pure N-GQDs solution was obtained.

2.4 Fluorescence detection for TYR activity

200 μL purified N-GQDs solution were placed in a series of 2.0 mL calibrated test tubes.

Subsequently, tyrosine (2.5 μmol L^{-1}), different amounts of TYR and 0.01 mol L^{-1} Tris-HCl buffer solution (pH 6.2) were added respectively. Then, the mixtures were diluted to 2.0 mL with deionized water and mixed thoroughly at 37°C for120 min. The fluorescence spectra were recorded in the 370-600 nm emission wavelength range at an excitation wavelength of 350 nm.

2.5 Fluorescence detection for ACP activity

AAP (30 μmol L^{-1}) and different amounts of ACP were mixed in a series of 2.0 mL calibrated test tubes at 37°C. 40 min later, 200 μL N-GQDs, tyrosine (2.5 μmol L^{-1}), TYR (3.85 U mL^{-1}) and 0.01mol L^{-1} Tris-HCl buffer solution (pH 6.2) were added into the above solutions. The mixtures were diluted to 2.0 mL with deionized water and then mixed thoroughly and incubated for 120 min at 37 °C. At an excitation wavelength of 350 nm, the fluorescence spectra were recorded in the 370-600 nm emission wavelength range.

2.6 Real sample assay

For the analysis of serum samples, drug-free human blood samples were collected from the university hospital. All the blood samples were obtained by venipuncture and centrifuged at 10000 rpm for 10 min at room temperature. The supernatant was separated and deproteinized by adding acetonitrile (CH_3CN) to the samples (CH_3CN: serum = 1:1). After vigorous shaking for 2 min, the mixture was centrifuged at 10000 rpm for 10 min at 4°C. The obtained supernatant was filtered twice. The filtrate was adjusted to neutral pH and then diluted 100-fold with deionized water. Different concentrations of TYR and ACP were added to the diluted serum samples to prepare spiked samples. Real sample analysis was carried out using the procedure described above.

3. Results and discussion

3.1 Characterization of N-GQDs

Fig. 1

The N-GQDs was systematically characterized by employing transmission electron microscopy (TEM), UV-vis spectroscopy, FT-IR spectrometry and fluorescence spectra, which were showed in Fig. 1. As shown in Fig. 1A and B, N-GQDs were well dispersed and showing the spherical morphology with the average diameter 2.8 nm. The functional groups on the surface of

N-GQDs were investigated using FT-IR spectrometry. As shown in Fig. 1C, absorption peaks at 3425 and 3215 cm^{-1} were characteristic absorption of O-H and N-H stretching vibration, respectively. Absorption peak at 1595 cm^{-1} was assigned to stretching vibration of C-N. Absorption peaks at 2968 and 2856 cm^{-1} correspond to C-H stretching vibration. Absorption peaks at 1332 and 1392 cm^{-1} were ascribed to the typical stretching vibration modes of C=N and C-N heterocycles [23]. Fig. 1D showed the N-GQDs exhibited the maximal emission at 450 nm (black line) under the excitation at 350 nm (red line), and the UV-vis absorption spectra of N-GQDs showed the strong absorbance at 345 nm which result from n-π* transition of C=O or C-OH bond in sp^3 hybrid regions, originates from the trapping of excited state energy of the surface states, which can lead to strong fluorescence [22]. Inset in Fig. 1D showed the photographic images of N-GQDs, the N-CQDs aqueous solution was colorless under ambient daylight and exhibited a very intense blue color when irradiated with UV light (365 nm), further indicating the blue fluorescent property of the N-CQDs. The strong fluorescence of the N-CQDs may result from the emissive traps of the nitrogen-doped surface [24]. These results indicated that N-GQDs with bright blue fluorescence were successfully obtained.

3.2 The design strategy for TYR and ACP detection

Fig. 2

As illustrated in Scheme 1, tyrosine could be catalyzed by TYR to generate dopaquinone, which could quench the fluorescence of N-GQDs significantly, while the fluorescence was recovered with the addition of AAP and ACP. In order to prove the feasibility of the strategy, the effect of different components on the fluorescence of N-GQDs was studied. As shown in Fig. 2, there was no significant change of the fluorescence of N-GQDs after mixed with tyrosine, TYR, AAP and ACP separately (Fig. 2A). After addition of tyrosine and TYR, the fluorescence of N-GQDs decreased greatly. And there was no significant change of the fluorescence of N-GQDs/tyrosine/TYR system after mixed with ACP. The fluorescence of N-GQDs/tyrosine/TYR system recovered a little after addition of AAP, which was due to the little reducibility of AAP. But after addition of ACP and AAP simultaneously, the fluorescence of N-GQDs recovered greatly.

In order to study the quenched fluorescence by dopaquinone could be recovered by AA, the

effect of different concentrations of AA on the fluorescence intensity of the N-GQDs/tyrosine/TYR system was studied. As shown in Fig. S1, the fluorescence intensity of the N-GQDs/tyrosine/TYR system gradually increased with the increase of the AA concentration. Inset in Fig. S1 illustrated a good linear relationship between I/I_0 and the concentration of AA in the range from 1-22.5 μmol L^{-1}, where I_0 and I stand for the fluorescence intensity of the N-GQDs/tyrosine/TYR system in the absence and presence of AA. All the results further proved the feasibility of the detection mechanism of the proposed method.

The fluorescence quenching of N-GQDs was considered to be related to the formation of o-quinone. Quinones were reported as an efficient fluorescence quencher for fluorescence probes such as QDs and noble metal NCs [25]. For further explanation of the mechanism, UV-vis absorption and fluorescence lifetime were studied. As shown in Fig. S2A, N-GQDs had an apparent emission peak at 450 nm, which could not be influenced by absorption peak of tyrosine at 275 nm. Under catalysis of TYR, tyrosine was oxidized into dopaquinone, which can serve as a good electron acceptor, and the absorption appeared at 275 nm decreased. Furthermore, the fluorescence decay curves for the N-GQDs in the absence and presence of dopaquinone were studied. The related data were given in Table S1. The decay curves for the N-GQDs with and without dopaquinone fitted well to the bi-exponential function. The fluorescence lifetime of N-GQDs (2.44 ns) was longer than that of N-GQDs/tyrosine/TYR (1.31 ns), implying that the dynamic quenching process was dominant for quenching mechanism. It proved that dopaquinone can efficiently quench the fluorescence of N-GQDs through the dynamic quenching process [26, 27].

3.3 Optimization for TYR and ACP detection

Fig. 3

In order to obtain a fluorescence biosensor with good sensing performance, we further optimized the experiment conditions. In this work, the concentration of tyrosine and the incubation time were investigated firstly. The effect of incubation time on the fluorescence of N-GQDs/tyrosine/TYR system was investigated in Fig. 3A. It can be seen that the fluorescence intensity the N-GQDs decreased to the minimum within 120 min and remained stable with further

increase of the reaction time. So, the optimal incubation time for TYR detection was chosen as 120 min. The effect of pH was investigated in the pH range of 6.2–9.0. As shown in Fig. 3B, the fluorescence intensity of N-GQDs almost kept stable in the pH range of 6.2-9.0, and the fluorescence intensity of N-GQDs/tyrosine/TYR and N-GQDs/tyrosine/TYR/AAP/ACP system increased with the increase of pH. It can be seen that the quenching efficiency and recovering efficiency were the maximum at pH=6.2. Moreover, the optimal ability for catalytic hydrolysis of ACP was observed in a low-pH environment. Therefore, a pH of 6.2 was chosen in the following experiments. The effect of tyrosine concentration on the fluorescence intensity of N-GQDs/tyrosine/TYR system was investigated. As shown in Fig. 3C, the fluorescence intensity of the N-GQDs decreased gradually with the increase of tyrosine concentration, so the fluorescence quenching effect of dopaquinone on N-GQDs increased gradually with increasing the concentration of tyrosine and then kept constant when the concentration of tyrosine was more than 2.5 μmol mL^{-1}. Thus, 2.5 μmol mL^{-1} tyrosine was chosen in the following experiments. The effect of incubation time (AAP and ACP) on the fluorescence intensity of N-GQDs/tyrosine/TYR/AAP/ACP system was shown in Fig. 3D. The fluorescence intensity of the system increased to the maximum within 30 min and remained stable with further increase of the incubation time. Thus，40 min was adopted as the reaction time between ACP and AAP in the following experiments.

3.4 Detection of TYR

Fig. 4

The fluorescence spectra of N-GQDs/tyrosine/TYR system with different concentrations of TYR under the optimum conditions were shown in Fig. 4A. It can be seen that the fluorescence intensity of the system was gradually decreased with the increase of TYR concentration. Fig. 4B illustrated a good linear relationship between I/I_0 (where I_0 and I stands for the fluorescence intensity of the N-GQDs/tyrosine/TYR system in the absence and presence of TYR) and the concentration of TYR, The linear relationships between the fluorescence intensity and the TYR concentration could be described as follows I/I_0=1.007-0.05047[TYR], U mL^{-1} for 0.43-2.14 U mL^{-1} TYR and I/I_0=1.797-0.4229[TYR], U mL^{-1} for 2.14-3.85 U mL^{-1} TYR, respectively. The

correlation coefficients were R^2 = 0.9567 and R^2 = 0.9975, respectively. The detection limit (LOD) was 0.15 U mL^{-1}. The detection limit was defined by the equation LOD=3σ/s, where σ was the standard deviation of the corrected blank signals and s was the slope of the calibration curve.

3.5 Detection of ACP

Fig. 5

The fluorescence spectra of the N-GQDs/tyrosine/TYR/AAP/ACP system with different concentrations of ACP were shown in Fig. 5A. It can be seen that the fluorescence intensity of the system gradually increased with the increase of the ACP concentration. Fig. 5B shown a good linear relationship between I/I_0 and the concentration of ACP (R^2=0.9994) in the range from 0.04 to 0.7 mU mL^{-1}. The linear regression equation was: I/I_0= 1.001+0.6321[ACP]，mU mL^{-1} with the detection limit of 0.014 mU mL^{-1}. It has been reported that the normal level of ACP in blood serum is in the range of 35 to 123 mU mL^{-1} [28]. Therefore, the present method was capable of detecting the activity of ACP in biological fluids.

3.6 Interference study

Fig. 6

To investigate the specificity of the biosensor for TYR and ACP, its selectivity was further evaluated using various interfering inorganic salts, metal ions, biological small molecule, proteins and enzymes, which were added to system under the same conditions, including K^+, Ca^{2+}, Mg^{2+}, cholesterol, glucose, tyrosine, tryptophan, arginine, threonine, phenylalanine，Human serum albumin (HSA), pepsin, trypsin, uricase, glucose oxidase and lysozyme. We studied the influences of various common coexisting substances to the detection of 3.12 U mL^{-1} TYR and 0.7 mU mL^{-1} ACP, respectively. As shown in Fig. 6A and B, common inorganic salts, metal ions and biomolecules (250-fold K^+, Ca^{2+}, Mg^{2+}, cholesterol, glucose, tyrosine, tryptophan, arginine, threonine and phenylalanine, 10-fold human serum albumin (HSA), pepsin, trypsin, uricase, glucose oxidase and lysozyme) had little effect on the fluorescence of N-GQDs/tyrosine/TYR and N-GQDs/tyrosine/TYR/AAP/ACP system, which was considered to be ignorable. The results

showed that common metal ions and biomolecules had no obvious interference on the detection of TYR and ACP, indicating that this method had a high selectivity toward TYR and ACP.

3.7 Real samples detection

In order to evaluate the feasibility of the proposed method in real sample analysis, the developed fluorescence biosensor was applied for the detection of TYR and ACP in human serum samples. The results obtained by a standard addition method were shown in Table S2 and Table S3, and the accuracy of the proposed method was measured by determining the recoveries of TYR and ACP in serum samples. It can be observed that the recoveries of TYR and ACP were in the range of 97% -106% and 96%-110%, respectively and the relative standard deviation (RSD) was lower than 2.65 and 3.98 for TYR and ACP, respectively. The above results demonstrated that the proposed method has potential application in real sample detection of TYR and ACP.

4. Conclusion

In conclusion, we have successfully developed a novel fluorescence biosensor for TYR and ACP activity detection based on N-GQDs. Tyrosine could be catalyzed by TYR to generate dopaquinone, which could efficiently quench the fluorescence of N-GQDs. In the presence of ACP, AAP could be hydrolyzed to generate reductive AA, which could reduce dopaquinone, and resulting in the recovery of the quenched fluorescence. Utilizing the change of fluorescence intensity, a novel, sensitive and selective fluorescence biosensor for TYR and ACP activity was constructed with the detection limits of 0.15 U mL^{-1} and 0.014 mU mL^{-1}, respectively. The method was successfully applied in real sample detection with satisfactory results and good repeatability.

Acknowledgments

This work was financially supported by the National Natural Science Foundation of China (No. 21275063 and No. 21575048), the Science and Technology Development project of Jilin province, China (No. 20150204010GX).

References

[1] X. Yan, T. Hu, L. Wang, L. Zhang, X. Su, Near-infrared fluorescence nanoprobe for enzyme-substrate system sensing and in vitro imaging, Biosensors & Bioelectronics 79 (2016) 922-929.

[2] H. Claus, H. Decker, Bacterial tyrosinases, Systematic And Applied Microbiology 29(1) (2006) 3-14.

[3] R. Yoruk, M.R. Marshall, Physicochemical properties and function of plant polyphenol oxidase: A review, Journal Of Food Biochemistry 27(5) (2003) 361-422.

[4] T.-S. Chang, An Updated Review of Tyrosinase Inhibitors, International Journal Of Molecular Sciences 10(6) (2009) 2440-2475.

[5] S. Halaouli, M. Asther, J.C. Sigoillot, M. Hamdi, A. Lomascolo, Fungal tyrosinases: new prospects in molecular characteristics, bioengineering and biotechnological applications, J. Appl. Microbiol. 100(2) (2006) 219-232.

[6] P. Garcia, I.A. Ramallo, R.L.E. Furlan, Reverse Phase Compatible TLC-Bioautography for Detection of Tyrosinase Inhibitors, Phytochem. Anal. 28(2) (2017) 101-105.

[7] 김혜린, Recent Advances in Tyrosinase Research as An Industrial Enzyme, Korean Society for Biotechnology and Bioengineering Journal 29(1) (2014) 1-8.

[8] T.G. Hastings, Enzymatic oxidation of dopamine: the role of prostaglandin H synthase, Journal of neurochemistry 64(2) (1995) 919-24.

[9] I. Tessari, M. Bisaglia, F. Valle, B. Samori, E. Bergantino, S. Mammi, L. Bubacco, The reaction of alpha-synuclein with tyrosinase - Possible implications for Parkinson disease, Journal Of Biological Chemistry 283(24) (2008) 16808-16817.

[10] H. Bull, P.G. Murray, D. Thomas, A.M. Fraser, P.N. Nelson, Acid phosphatases, Journal Of Clinical Pathology-Molecular Pathology 55(2) (2002) 65-72.

[11] E.S. Leman, R.H. Getzenberg, Biomarkers for Prostate Cancer, Journal Of Cellular Biochemistry 108(1) (2009) 3-9.

[12] C.Y. Li, L.T. Yam, K.W. Lam, Acid phosphatase isoenzyme in human leukocytes in normal and pathologic conditions, The journal of histochemistry and cytochemistry : official journal of the Histochemistry Society 18(7) (1970) 473-81.

[13] E. Schiffer, Biomarkers for prostate cancer, World Journal Of Urology 25(6) (2007) 557-562.

[14] A.H. Kamel, H.R. Galal, A.A. Hanna, Novel Planar Chip Biosensors for Potentiometric Immunoassay of Acid Phosphatase Activity Based on the Use of Ion Association Complexes as Novel Electroactive Materials, International Journal Of Electrochemical Science 9(10) (2014) 5776-5787.

[15] Y. Yamauchi, M. Ido, H. Maeda, High performance liquid chromatography equipped with a cathodic detector and column-switching device as a high-throughput method for a phosphatase assay with p-nitrophenyl phosphate, Journal Of Chromatography A 1066(1-2) (2005) 127-132.

[16] P. Calvo-Marzal, S.S. Rosatto, P.A. Granjeiro, H. Aoyama, L.T. Kubota, Electroanalytical determination of acid phosphatase activity by monitoring p-nitrophenol, Analytica Chimica Acta 441(2) (2001) 207-214.

[17] Y. Xu, B. Li, P. Han, S. Sun, Y. Pang, Near-infrared fluorescent detection of glutathione via reaction-promoted assembly of squaraine-analyte adducts, Analyst 138(4) (2013) 1004-1007.

[18] S. Wu, X. Gao, Q. Cai, C.A. Grimes, A wireless magnetoelastic biosensor for convenient and sensitive detection of acid phosphatase, Sensors And Actuators B-Chemical 123(2) (2007) 856-859.

[19] Z.S. Qian, L.J. Chai, Q. Zhou, Y.Y. Huang, C. Tang, J.R. Chen, H. Feng, Reversible Fluorescent Nanoswitch Based on Carbon Quantum Dots Nanoassembly for Real-Time Acid Phosphatase Activity Monitoring, Analytical Chemistry 87(14) (2015) 7332-7339.

[20] T. Fan, W. Zeng, W. Tang, C. Yuan, S. Tong, K. Cai, Y. Liu, W. Huang, Y. Min, A.J. Epstein, Controllable size-selective method to prepare graphene quantum dots from graphene oxide, Nanoscale Research Letters 10 (2015) 1-8.

[21] Y. Wang, R. Hu, G. Lin, I. Roy, K.-T. Yong, Functionalized Quantum Dots for Biosensing and Bioimaging and Concerns on Toxicity, Acs Applied Materials & Interfaces 5(8) (2013) 2786-2799.

[22] Y. Zhang, P.P. Cui, F. Zhang, X.T. Feng, Y.L. Wang, Y.Z. Yang, X.G. Liu, Fluorescent probes for "off-on" highly sensitive detection of Hg^{2+} and L-cysteine based on nitrogen-doped carbon dots, Talanta 152 (2016) 288-300.

[23] J. Ju, R. Zhang, S. He, W. Chen, Nitrogen-doped graphene quantum dots-based fluorescent probe for the sensitive turn-on detection of glutathione and its cellular imaging, Rsc Advances 4(94) (2014) 52583-52589.

[24] R. Zhang, W. Chen, Nitrogen-doped carbon quantum dots: Facile synthesis and application as a "turn-off' fluorescent probe for detection of Hg^{2+} ions, Biosensors & Bioelectronics 55 (2014) 83-90.

[25] C. Burda, T.C. Green, S. Link, M.A. El-Sayed, Electron shuttling across the interface of CdSe nanoparticles monitored by femtosecond laser spectroscopy, J. Phys. Chem. B 103(11) (1999) 1783-1788.

[26] X. Zhu, J. Hu, Z. Zhao, M. Sun, X. Chi, X. Wang, J. Gao, Kinetic and Sensitive Analysis of Tyrosinase Activity Using Electron Transfer Complexes: In Vitro and Intracellular Study, Small 11(7) (2015) 862-870.

[27] Y. Teng, X.F. Jia, J. Li, E.K. Wang, Ratiometric Fluorescence Detection of Tyrosinase Activity and Dopamine Using Thiolate-Protected Gold Nanoclusters, Analytical Chemistry 87(9) (2015) 4897-4902.

[28] S.S.M. Hassan, H.E.M. Sayour, A.H. Kamel, A simple-potentiometric method for determination of acid and alkaline phosphatase enzymes in biological fluids and dairy products using a nitrophenyl phosphate plastic membrane sensor, Analytica Chimica Acta 640(1-2) (2009) 75-81.

Captions:

Scheme 1. Schematic illustration of the novel biosensor for TYR and ACP detection.

Fig. 1 (A) The TEM image of N-GQDs and (B) the size distribution of N-GQDs; (C) FT-IR spectra of the N-GQDs; (D) UV-vis absorption and fluorescence excitation and emission spectra of N-GQDs; The inset of (D) is the images of N-GQDs solution taken under visible light (left) and 365 nm UV light (right).

Fig. 2 (A) Fluorescence emission spectra of N-GQDs, N-GQDs/tyrosine, N-GQDs/TYR, N-GQDs/AAP and N-GQDs/ACP system; (B) Fluorescence emission spectra of N-GQDs/tyrosine/TYR, N-GQDs/tyrosine/TYR/ACP, N-GQD/tyrosine/TYR/ACP and N-GQDs/tyrosine/TYR/AAP/ACP system.

Fig. 3 (A) Effect of incubation time on the fluorescence intensity of the N-GQDs/tyrosine/TYR system; (B) Effect of pH on the fluorescence intensity of N-GQDs (black squares), N-GQDs/tyrosine/TYR (red dots) and N-GQDs/tyrosine/TYR/AAP/ACP system (blue triangles); (C) Effect of tyrosine concentration on the fluorescence intensity of N-GQDs/tyrosine/TYR system; (D) Effect of incubation time (AAP and ACP) on the fluorescence intensity of N-GQDs/tyrosine/TYR//AAP/ACP system.

Fig. 4 (A) Fluorescence spectra of the N-GQDs/tyrosine/TYR system with different concentrations of TYR (curves a to i represents concentrations of 0, 0.43, 0.86, 1.71, 2.14, 2.57, 2.99, 3.42 and 3.85 U mL^{-1}); (B) Plot of the relative fluorescence intensity (I/I_0) of the N-GQDs/tyrosine/TYR system against the TYR concentration, where I_0 and I stand for the fluorescence intensity of the N-GQDs/tyrosine/TYR system in the absence and presence of TYR.

Fig. 5 (A) Fluorescence spectra of the N-GQDs/tyrosine/TYR/AAP/ACP system with different concentrations of ACP (curves a to j represents concentrations of 0, 0.04, 0.1, 0.15, 0.2, 0.3, 0.4, 0.5, 0.6, 0.7 mU mL^{-1}) ; (B) Plot of the relative fluorescence intensity (I/I_0) of the N-GQDs/tyrosine/TYR/AAP/ACP system against the ACP concentration, where I_0 and I stand for the fluorescence intensity of the N-GQDs/tyrosine/TYR/AAP system in the absence and presence of ACP. Tyrosine (2.5 μmol mL^{-1}), TYR (3.85 U mL^{-1}) and AAP (30 μmol L^{-1})

Fig. 6 (A) The fluorescence intensity of the N-GQDs/tyrosine/TYR system with the interfering substances (250-fold for K^+, Ca^{2+}, Mg^{2+}, cholesterol, glucose, tyrosine, tryptophan, arginine, threonine and phenylalanine, 10-fold for human serum albumin (HSA), pepsin, trypsin, uricase,

glucose oxidase and lysozyme) and (B) the fluorescence intensity of the N-GQDs/tyrosine/TYR/AAP/ACP system with the interfering substances (250-fold for K^+, Ca^{2+}, Mg^{2+}, cholesterol, glucose, tyrosine, tryptophan, arginine, threonine and phenylalanine, 10-fold for human serum albumin (HSA), trypsin, uricase, glucose oxidase and lysozyme)

Figures:

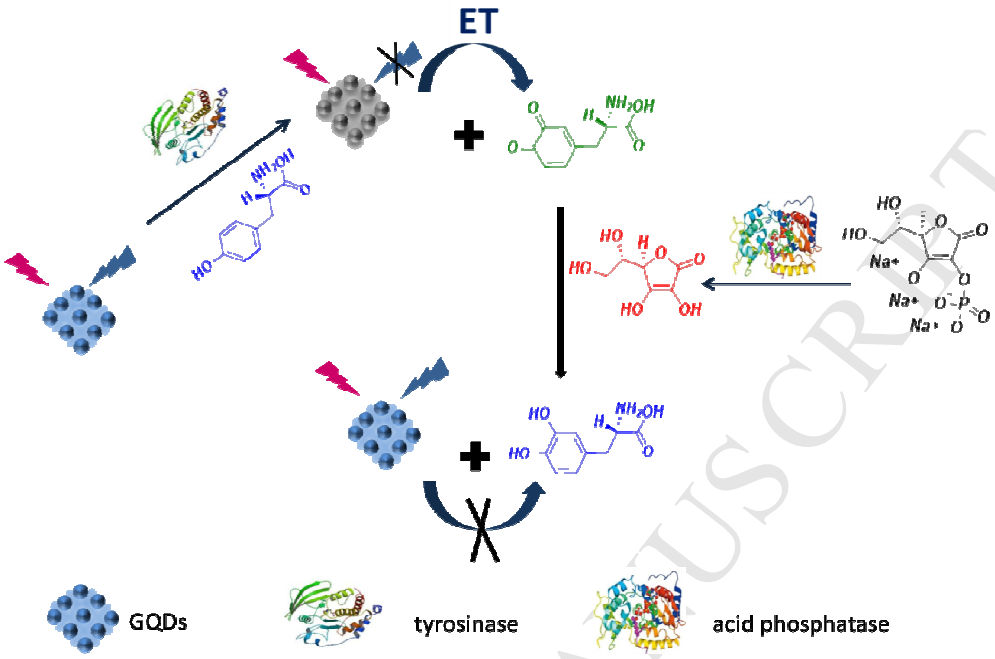

Scheme 1

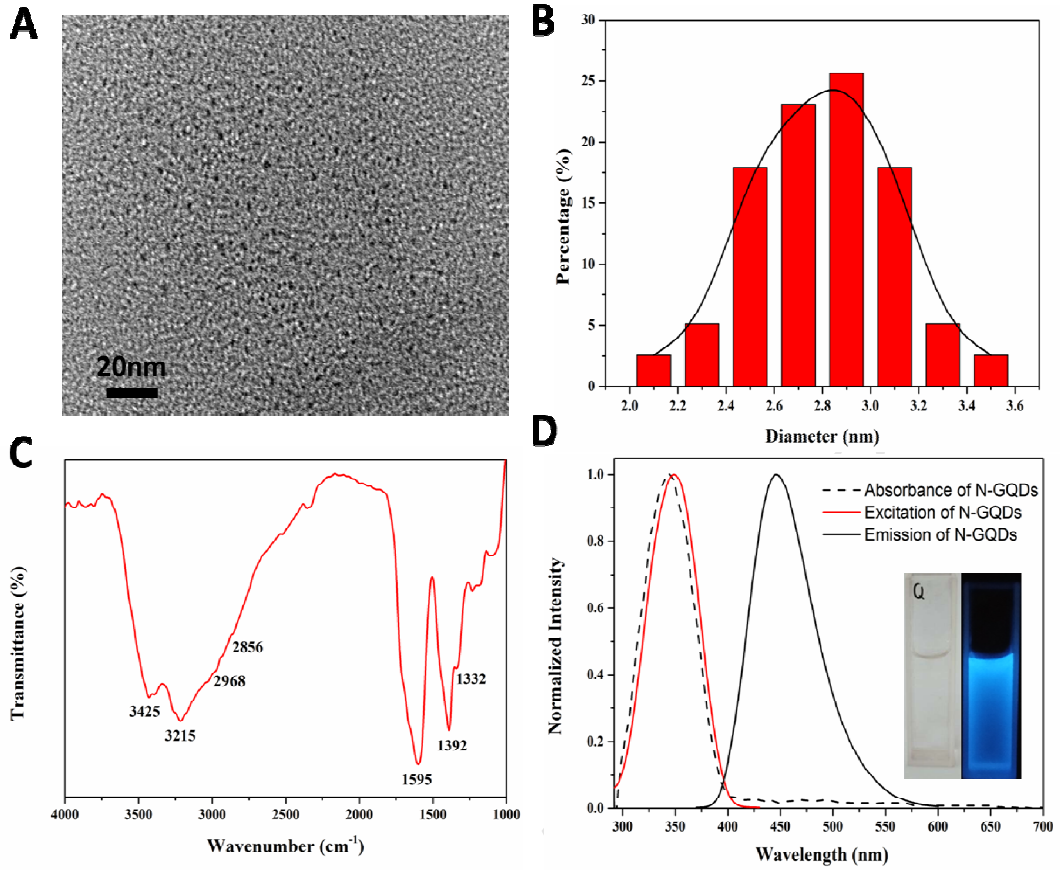

Fig. 1

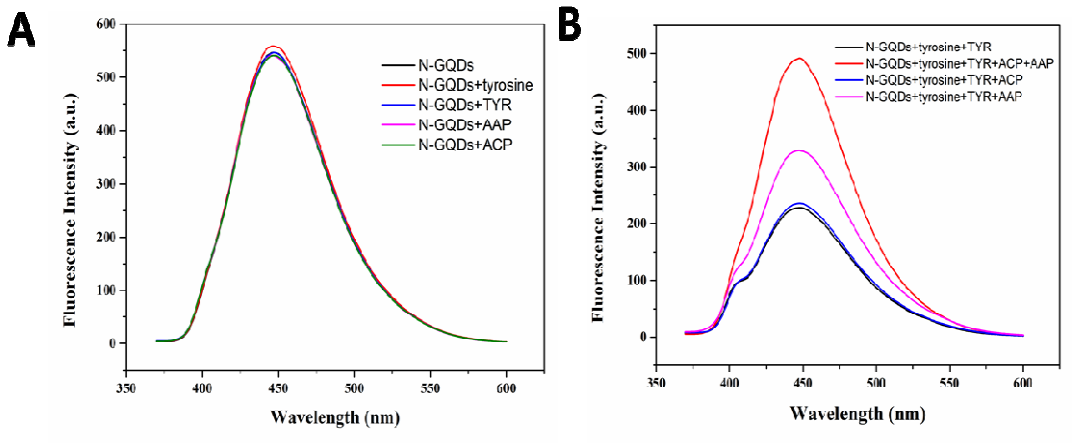

Fig. 2

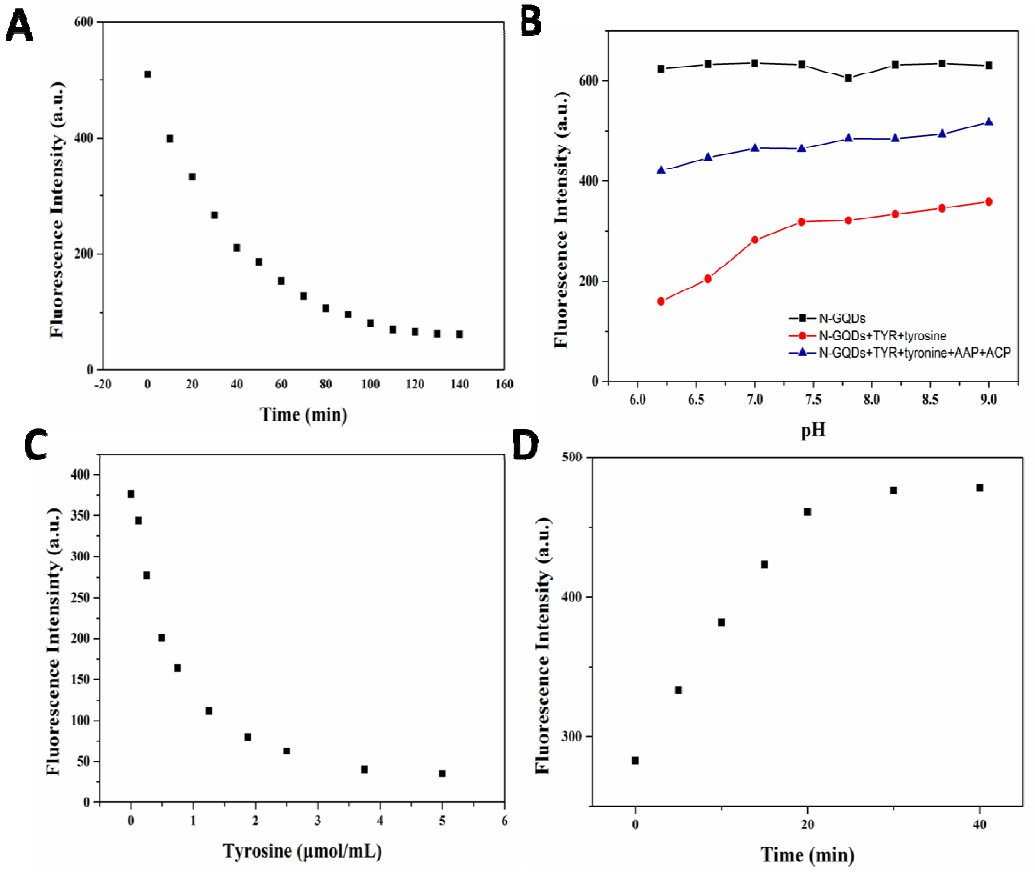

Fig. 3

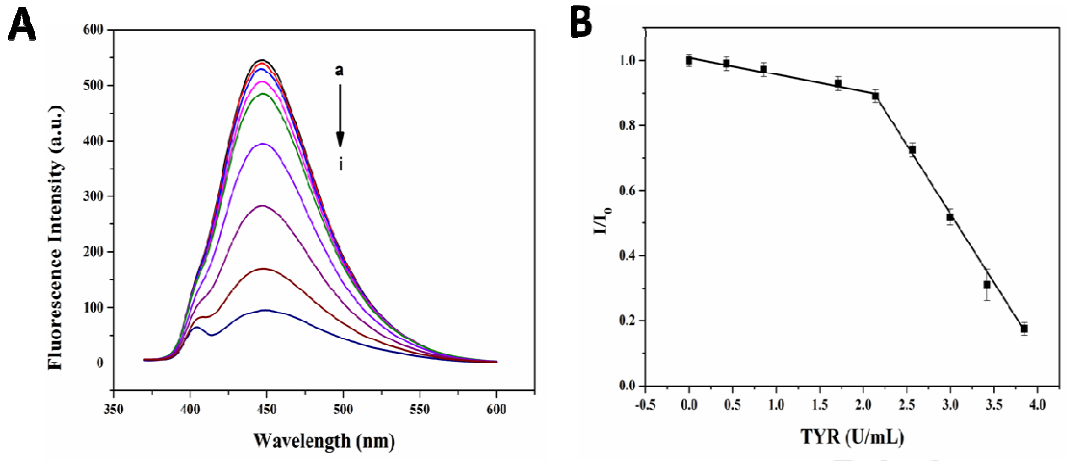

Fig. 4

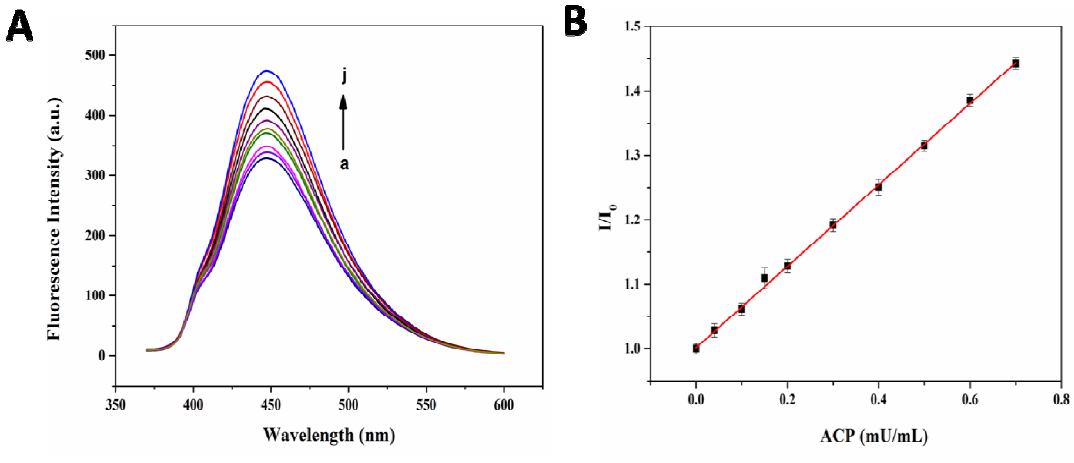

Fig. 5

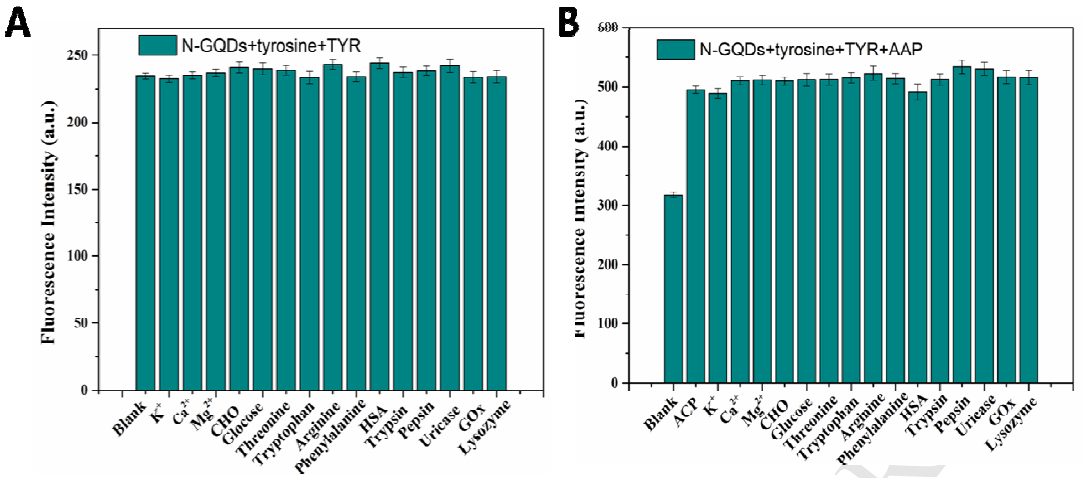

Fig. 6

Highlights:

► Strongly fluorescent N-GQDs were successfully prepared by hydrothermal method

► A novel fluorescent biosensor for label-free detection of TYR and ACP was established based on the N-GQDs.

► Good sensitivity and selectivity were obtained.

► This method was utilized to detect TYR and ACP in real sample with satisfactory results.